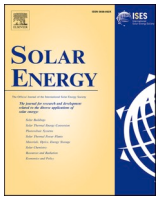
Solar Energy 297 (2025) 113609



Contents lists available at ScienceDirect

Solar Energy

journal homepage: www.elsevier.com/locate/solener





Sustainable solution for direct absorption of solar thermal energy in biochar-based form stable thermal energy storage media for low radiation regions by integration of Cross Compound Parabolic Concentrator

Dudul Das, Manosh C. Paul *

Systems, Power & Energy Research Division, James Watt School of Engineering, University of Glasgow, UK

ARTICLE INFO

Keywords:
Latent heat energy storage
Solar concentrator
Form stable phase change material
Biochar
Heat transfer

ABSTRACT

Renewable energy to meet the low temperature thermal needs is need of the hour as it contributes to almost half of the consumption. The adoption of thermal energy storage can accelerate the share of renewable heat by improving reliability and efficiency. A novel thermal energy storage material is developed by encapsulating paraffin-based Phase Change Material (PCM) in porous biochar to improve thermal conductivity and prevent leakage. This composite is then placed in a rectangular cavity and radiated using a halide light source from top to mimic the actual solar heating. To reach a high level of irradiance a Cross Compound Parabolic Concentrator (CCPC) with a concentration of 4× has been designed and utilised. The work includes a comparative study of pure RT28 and RT28-softwood biochar composite. A solution is proposed to advance the applicability of latent heat energy storage, charged through direct solar absorption, by use of a well-designed CCPC under low radiation conditions. The composite with concentration melts 5.4 times faster as compared to non-concentration condition. Similarly, the melting is quicker in the composite as that of RT28 due to improvement of thermal conductivity by 80 %. CCPC integrated thermal energy storage can reach an average storage temperature of 89.7 °C with an irradiance of 540 W/m^2. These findings could be helpful to accelerate the deployment of PCM based biochar composite for energy storage applications in the locations with low solar irradiance and short sunshine duration.

1. Introduction

The depleting fossil fuel reserves and deteriorating climate has created several economical and ethical questions [1]. A clean, reliable and adequate energy supply is essential for the sustainability of modern societies [2]. However, at present the fossil fuel dominated energy generation has been unsuccessful to meet this demand. Heat makes up half of the world's total final energy consumption, yet only a quarter of it comes from renewable sources. This could be a sensible strategy to decarbonise this sector to achieve a net zero future by making the maximum possible use of renewable thermal energy sources. This will improve their reliability and supply continuity by the deployment of suitable Thermal Energy Storage (TES) solutions. Among the available technologies latent heat storage is the most preferred in this temperature bracket. Latent heat storage, compared to sensible heat storage, has almost 5–14 times greater energy storage density, without a significant increase in cost [3]. From a material standpoint, paraffins, as a PCM, have been recognised for avoiding common issues such as supercooling, corrosion, and phase separation [4]. However, poor thermal conductivity and the issue of liquid leakage during phase transitions have come out as two major drawbacks.

One effective approach to improving the form stability and thermal performance of PCMs is by incorporating a supporting matrix, which offers mechanical support as well as containment, thus preventing leakage while ensuring long-term stability [5]. Important factors to consider when choosing a supporting matrix for PCMs include compatibility with materials, mechanical strength, thermal conductivity, durability, aptness for production processes, chemical stability, and cost efficiency [6–7]. Qiu et al. introduced a multifunctional composite PCM leveraging balsa wood's hierarchical structure. This composite inspired by the powerful human muscle system and developed via in-situ polymerisation of polyurethane in the wood. This wood-based PCM could reach a tensile strength of 96.5 MPa along the longitudinal direction, up to 3–50 times that of the reported PCMs, due to a unique aligned fiber array and energy dissipation system. Meanwhile, this composite had a high enthalpy of 95.4 J/g and a photothermal conversion efficiency of 83.2 % [8].

* Corresponding author.
E-mail address: Manosh.Paul@glasgow.ac.uk (M.C. Paul).

https://doi.org/10.1016/j.solener.2025.113609
Received 17 February 2025; Received in revised form 6 May 2025; Accepted 14 May 2025
Available online 20 May 2025
0038-092X/© 2025 The Author(s). Published by Elsevier Ltd on behalf of International Solar Energy Society. This is an open access article under the CC BY license (http://creativecommons.org/licenses/by/4.0/).

Nomenclature

Symbols

f	Focal length of the Cross Compound Parabolic Concentrator
C_g	Geometric concentration ratio
H	Height of the Cross Compound Parabolic Concentrator
W_{abs}	Receiver width in mm
W_{aper}	Aperture/entry width of the Cross Compound Parabolic Concentrator in mm
θ_c	Half acceptance angle of the concentrator

Abbreviations

BET	Brunauer, Emmett, and Teller
BPC	Biological Porous Carbon
CCPC	Cross Compound Parabolic Concentrator
DSC	Differential Scanning Calorimetry
FTIR	Fourier-transform infrared
LHTES	Latent Heat Thermal Energy Storage
MFPC	Metal Foam-PCM Composite
PCM	Phase Change Material
PEG	Polyethylene Glycol
TES	Thermal Energy Storage
XRD	X-ray powder diffraction

A study from India [9] reported eicosane and biopolymer based green composite for thermal energy storage in buildings. Incorporating modified n-eicosane into Poly (3-hydroxybutyrate-co-3-hydroxyvalerate) enhances shape stability and energy storage capacity, with corona-treated films achieving a high enthalpy of 184.9 ± 12.8 J/g and excellent thermal reliability. The optimal phase change temperature range (21–45 °C) aligns well with ambient conditions. Real-world testing in Delhi demonstrated a significant temperature reduction (~7.5 °C) in treated bricks, validating the material's passive thermal regulation capabilities.

Porous carbonaceous supporting materials found to be popular among the researchers due to its ability to improve thermal characteristics of the composite. A host work has been conducted to find out the suitable material to be used as supporting material. Adding graphite, graphene, or carbon nanotubes to PCM not only helps maintain its shape but also improves thermal conductivity by creating efficient heat transfer pathways [10]. While these advanced materials exhibit exceptional properties, but costly for large-scale commercial adoption. Biochar, one of the more established and cost-effective carbonaceous porous materials, remains a viable option for use in form-stable PCM production.

Liu et al. carried out a comparative study of different typical organic form-stable PCMs (lauric acid, hexadecanol and paraffin wax) packaged by carbonised wheat straw-expanded graphite binary supporting material [11]. DSC results showed that the enthalpy value of phase change was highest for wheat straw-expanded graphite/hexadecanol at 162.77 J/g and thermal conductivity of the wheat straw-expanded graphite/paraffin composite. The thermal conductivity significantly increased to 2.01 W/m K, a 615.1 % improvement over pure paraffin. Atinafu et al. [12] formulated an environmentally friendly, shape-stabilized, organic composite PCM using n-eicosane combined with wheat softwood and straw biochar, produced at pyrolysis temperatures of 550 °C and 700 °C. As the pyrolysis temperature increased, the surface area of softwood biochar exhibited an increase from 7.3 to 11.9 m^2/g. Das et al. [5,13] investigated the potential of using biochar produced from water hyacinth to develop a form-stable PCM based storage that could be effectively utilised to generate hot air under isothermal conditions for the drying of high-value agricultural products.

Study of heat transfer storage systems has been done by numerous researchers. Akyurek and Yoladi [14] conducted an experimental study on a cylinder containing RT50 as PCM, with heat transfer fluids circulating through channels of extremely small mini-channel diameters. The research focused on analysing the melting and solidification behaviour of RT50 while evaluating the impact of key parameters, including the temperature variation of fluid, channel diameter, and flow rate, on PCM TES. Metal foam found to significantly influences solid/liquid phase change during heat transfer, especially within the solid region of PCMs. During the melting process, natural convection enhances heat transfer, reducing the temperature gradient between the wall and the PCM. Joshi and Rathod [15] enhanced the thermal performance of a LHTES system by strategically incorporating a metal foam-PCM composite. Zhang et al. [16] studied the effects of structural parameters of metal foam (Copper and iron foams), and configurations of heating on the characteristics of heat transfer and melting process of PCM in large cavities. Metal foam with high thermal conductivity and low pore density was found to be the most effective in enhancing the melting process. Crosby et al. [17] for the first time modelled and numerically studied the performance of the melting process in a biochar-based PCM storage system. The melting time was reduced by 79 % with the use of SW-biochar, attributed to the enhanced thermal conductivity of the composite, even though heat transfer shifted from convective to conductive mechanisms.

The literature review reveals a scarcity of experimental investigations into form-stable materials incorporating carbonaceous support matrices when subjected to concentrated radiation. Most of the works are related to the characterisation and analysis of such novel composites. Few systems level experimental studies of composites of PCM and metal foam exists, but studies on micro or nanoporous carbonaceous supporting material-based composite is absent. It has been observed that biochar supported PCM has several advantages both in terms of physical and thermal properties. Thus, it can be used effectively for direct absorption of solar heat. Additionally, biochar improves the absorptivity of PCM material and helps in better radiation absorption. However, there is limited literature on experimental investigation of thermal energy storage with biochar supported form stable PCM. TES systems generally consist of shell side filled with PCM material while heat transfer fluid flows inside the tubes. Here, a system has been proposed where charging of the system will be through direct absorption of solar radiation. But such scheme has a geographic limitation. Such systems could not be easy to operate in the areas with a low solar irradiance value and system will take longer or in limiting case will not be charged fully. Thus, a proper concentrator can help to intensify the radiation to operate the TES to its full potential. Present work is an intersection of three components, (a) development and characterisation of softwood biochar and RT28 PCM composites, (b) design and fabrication of CCPC and (c) analysis of the melting behaviour of the softwood-RT28 composite in a rectangular cavity under elevated radiation level using a well-designed CCPC. Individual component has its own significance, development of form stable composite is necessary to get rid of inherent drawbacks of pure PCM such as low thermal conductivity and leakage. While CCPC integration to thermal energy storage unit could significantly widen the applicability even in regions with low solar irradiance level such as Europe, Canada, and Nordic regions. In these regions, TES has a maximum possible use ranging from space heating to domestic hot generation.

2. Material development, concentrator design, and experimental methodology

This section outlines three principal components of the present study. First, the development of a form-stable phase change material (PCM) composite is described, involving the integration of RT28 with softwood biochar. The characterisation techniques employed to assess the key thermophysical properties are also detailed. Next, a design methodology for the solar concentrator is presented. Finally, the thermal

Table 1
Characteristics of softwood biochar [18].

Parameter	Value
C_{total} (wt% dry basis)	90.21
H (wt% dry basis)	1.83
H:C_{total} (Molar ratio)	0.24
O (by difference) (wt% dry basis)	6.02
Total ash (wt% dry basis)	1.89
Total N (wt% dry basis)	0.1
pH	8.44
Electric conductivity	0.16

performance of the PCM composite is experimentally investigated within a rectangular cavity.

2.1. Form stable PCM- development and characterisation

The biochar produced from softwood at 700 °C is used as a supporting matrix in this study. The biochar was produced in a pilot-scale rotary kiln pyrolyser at the UK Biochar Research Centre (University of Edinburgh) [18]. The characteristic of the produced biochar is presented in Table 1.

Surface and pore characteristics of the biochar obtained from Brunauer, Emmett, and Teller (BET) study are shown in Fig. 1. As reported in a previous study [19], a blend of softwood biochar and RT28 (base PCM) in equal mass percentage is placed at a temperature of 35 °C for 16 h to get the leakproof form stable composite.

The biochar's morphological characteristics and porous nature have been evaluated using a BET surface area analyser (Quadrasorb EVO/SI). Crystallinity and chemical compatibility have been studied by XRD (Rigaku MiniFlex) and FTIR spectroscopy (JASCO). The crucial thermal parameters such heat of fusion and melting point is investigated by DSC (TA instruments DSC 25). The detailed elaboration of the characterisation techniques was already well presented by Das et al. [19].

Another important parameter for a thermal energy material for absorption of sunlight is photothermal conversion efficiency. To experimentally arrive at this performance parameter, the composite material and the pure PCM are positioned within rectangular cavities with transparent acrylic sheet of 3 mm thickness at the top to make radiation flux reach the material. The radiation intensity is validated using a radiometer. Once the temperature of each block reaches a specific threshold, the simulated solar light source is switched off, permitting natural cooling. The temperature fluctuations of each composite block are monitored and recorded using a data logger, as illustrated in Fig. 2. The efficiency of solar-thermal energy conversion, denoted as η_{st} can be computed using the subsequent equation [20],

$$\eta_{st} = \frac{m\Delta H_m}{GA(t_o - t_f)} \quad (1)$$

Where m is the mass of the PCM composite sample, ΔH_m is the melting enthalpy of the composite, G is the light intensity of the simulated sunlight, A is the area of the sample exposed to the radiation, and t_o and t_f are the times of the start and end of phase transition, respectively. The radiation at the surface of the cavity has been calculated to be 1998 W/m^2.

2.2. Cross compound parabolic concentrator (CCPC) design

The design methodology of a CCPC for applications in thermal energy storage systems is crucial, as it determines the level of concentration and size of the overall system. The key design parameters for CCPC are geometrical concentration (calculated using Eq. (1)), absorber width, half acceptance angle and concentrator height [21]. In this study, receiver size of 50 mm × 50 mm and geometric concentration ratio of 4 have been fixed (Fig. 2). The chosen concentration ratio reflects a balance between the design feasibility and maximised solar radiation

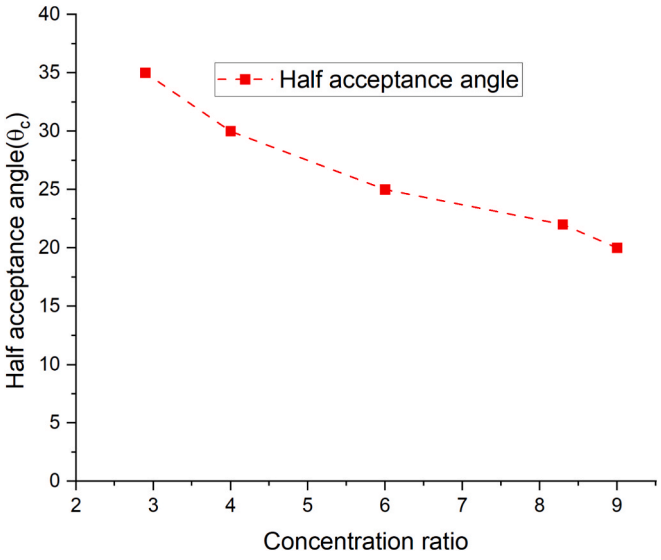


Fig. 2. Variation of concentration ratio with acceptance angle.

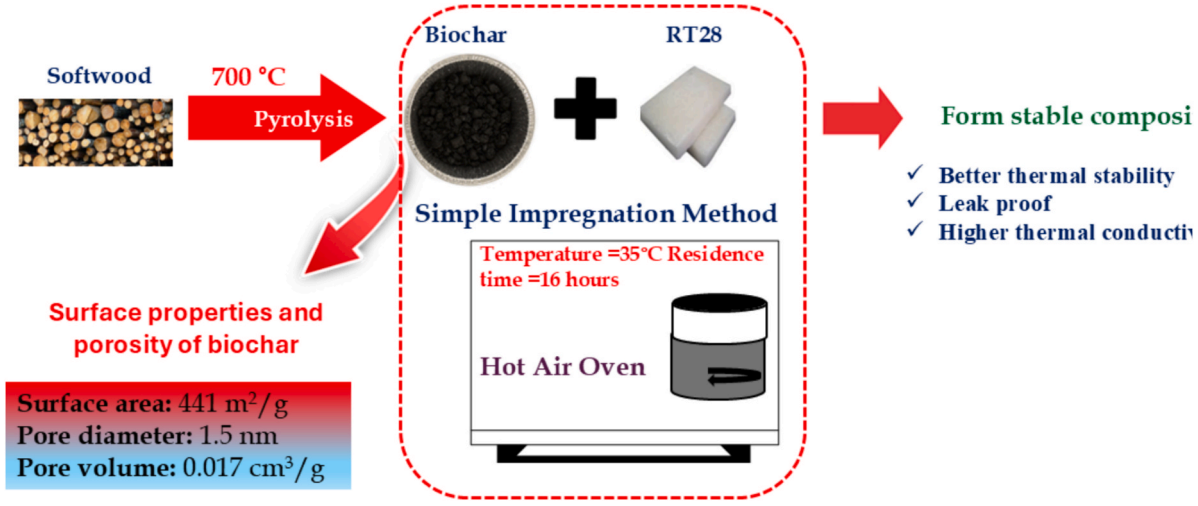


Fig. 1. Process of producing form stable composite PCM.

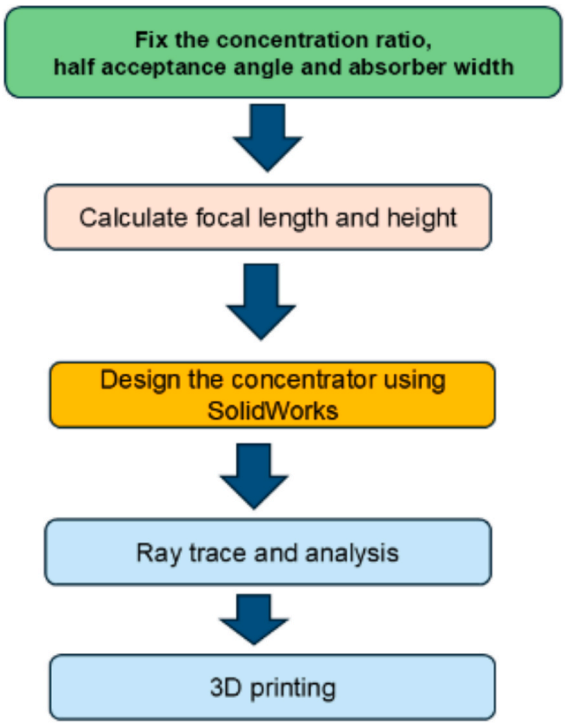


Fig. 3. Design steps of the CPCC.

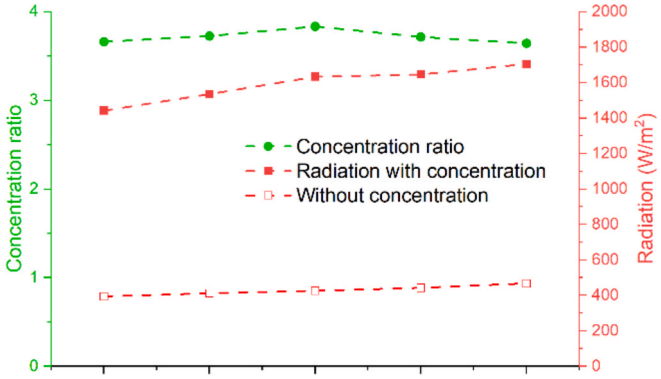


Fig. 4. Radiation at the receiver plane with and without CPCC.

interception. The optical concentration ratio, which is inherently lower than the geometrical ratio due to optical losses, was determined experimentally, as shown in Fig. 4. The average optical concentration ratio obtained from a series of experiments was 3.7, which closely aligns with the designed value.

Fig. 3 shows the design steps of CCPC. The following equations are used to find out the geometric concentration ratio (C_g), focal length (f) and height (H) of CCPC [21–24].

$$C_g = \frac{W_{aper}}{W_{abs}} \tag{2}$$

$$f = 0.5W_{abs}(1 + sin\theta_c) \tag{3}$$

$$H = f\frac{cos\theta_c}{sin^2\theta_c} \tag{4}$$

SolidWorks software is utilised to generate designs for 3D printing. Geometrical concentration ratio of 4x has been selected in this case. SolidWorks require two parameters to generate the CCPC parabolic curve – the half-acceptance angle (0.5236 rad) and the receiver size (50 mm). The coordinates $x(t)$ and $y(t)$, for the CCPC curves, are determined as

$$x(t) = \frac{W_{abs}(1 + sin\theta_c)cost}{1 - \sin(t - \theta_c)} \tag{5}$$

$$y(t) = \frac{W_{abs}(1 + sin\theta_c)sint}{1 - \sin(t - \theta_c)} \tag{6}$$

where W_{abs} is the receiver width in mm and t determines the curvature of the parabolic curve from the half acceptance angle,

$$t = \frac{\pi}{2} - \theta_c \tag{7}$$

In the case of a 4.0× concentrator, t_1 and t_2 are 0 and $\pi/2$ – 0.5236, respectively. Once the parametric equations are solved, parabolic curve for the concentrator is obtained.

The designed concentrator, as shown in Fig. 5, has been evaluated using TracePro to check the optical efficiency. An optical efficiency of 92.8 % has been found for the CCPC designed in this study whereas for the same source and receiver without concentrator the efficiency is 27 %, and this can be seen from Fig. 6. After all these steps, the designed CCPC is printed using Ultimaker 3D printer. Followed by printing, the inner surfaces of the CCPC is covered with reflecting mirror sheets.

2.3. Experimental study of PCM composite in rectangular cavity

PCM composite and pure RT 28 has been placed in a separate cavity

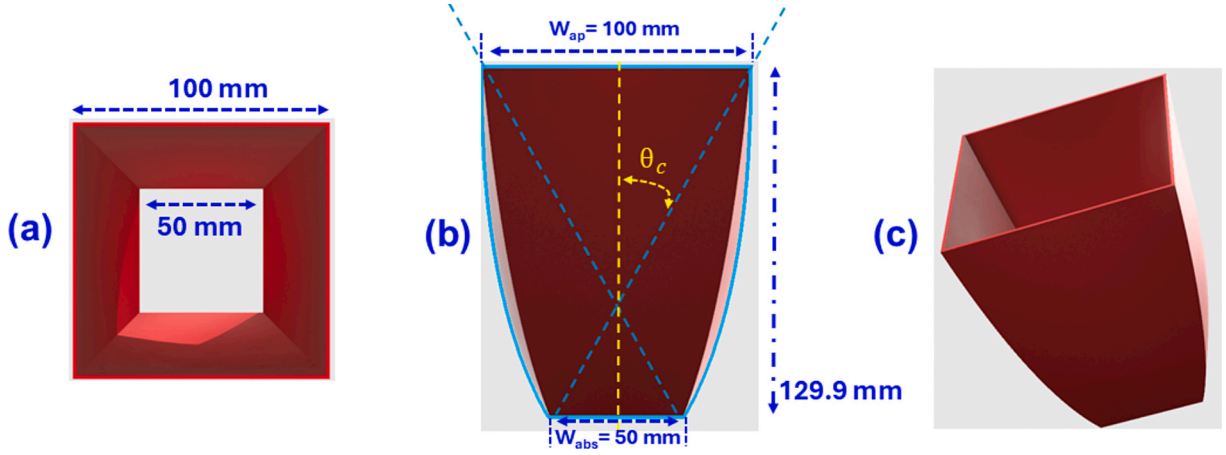


Fig. 5. Different views of designed CPCC (a) top view with dimensions of entry and exit; (b) side view; (c) inclined view.

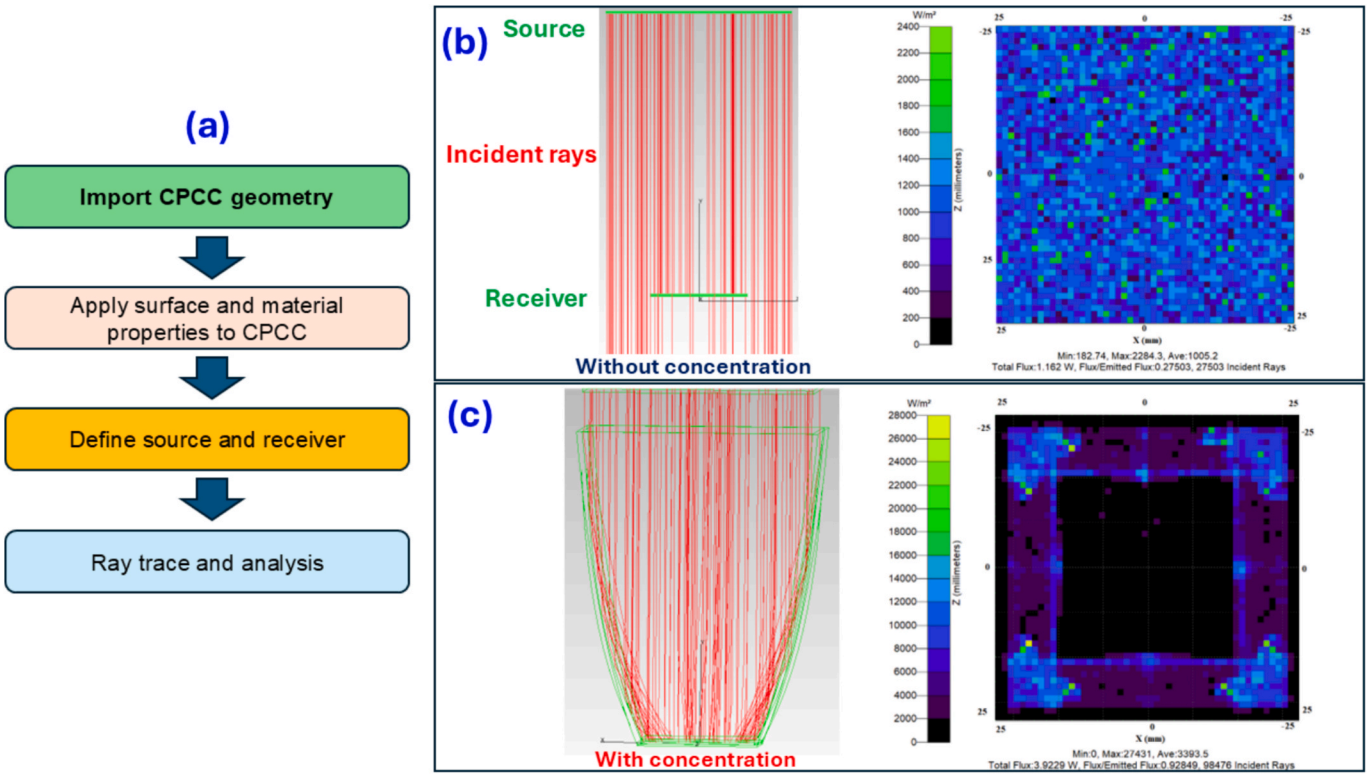


Fig. 6. TracePro analysis, (a) steps of concentrator simulation; (b) without CPCC; (c) 4.0x CCPC with reflector at 1000 W/m^2.

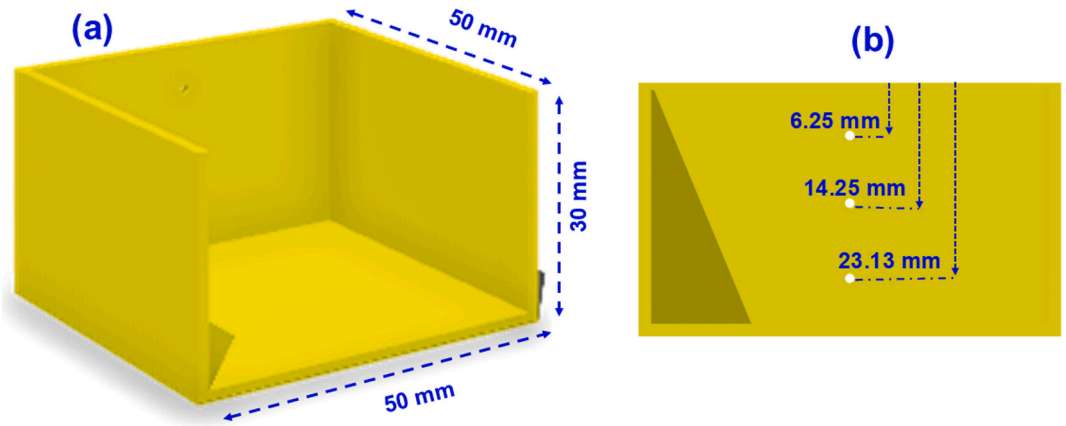


Fig. 7. Cavity for placing the PCM, (a) Dimensions; (b) Position of the holes to insert thermocouples.

as shown in Fig. 7. K-type thermocouples have been placed at different heights and in the direction of incoming radiation. CCPC is placed above the cavity (as shown in Fig. 8), the top and front surfaces of the cavity are made of 3 mm thick transparent acrylic glass. This allows maximum radiation to enter the cavity and to be absorbed by the storage medium. The transparent front surface allows an easy visualisation of the phase change process and a more critical evaluation using Infrared Imaging.

In this study, a rectangular cavity, that is filled with a PCM and subjected to top radiation flux, is investigated. Fig. 8 shows the schematic of the experimental setup used to obtain the information about melting behaviour of the pure PCM and composite. It consists of a rectangular cavity filled with form stable PCM with CCPC on the top, the radiation source, thermocouples connected to the data logger (Pico Technology USB TC-08) and the IR camera (FLIR A700) to record temperature contours. A gap of 2 mm is left from the top surface of the enclosure and top surface of the PCM material for accommodating volume expansion during the phase transition, which is generally 12.5 % for the RT28. In the experiment, K-type thermocouples were placed on the mid vertical plane of the rectangular cavity. The temperature contour of the enclosure is also captured from one side. An artificial light source is used as radiation source to heat the material from the top.

The experiment is carried out at three different levels to mimic different climates. The radiation level is adjusted by changing the height of the platform where the cavity is placed. In each height or radiation level behaviour of the material is studied under concentration and non-concentration conditions. The duration of charging is kept constant at 120 min for all cases. The three radiation levels are represented as L1, L2, and L3 with the radiation values of 330 W/m^2, 446 W/m^2, and 540 W/m^2 respectively. This value of radiation is before placing the CCPC. Shading experiment is a key part of this study. Blocking screen of area equivalent to 25 %, 50 % and 75 % of the entry area of the CCPC has been made and placed one by one. The screen is made brown thick paper

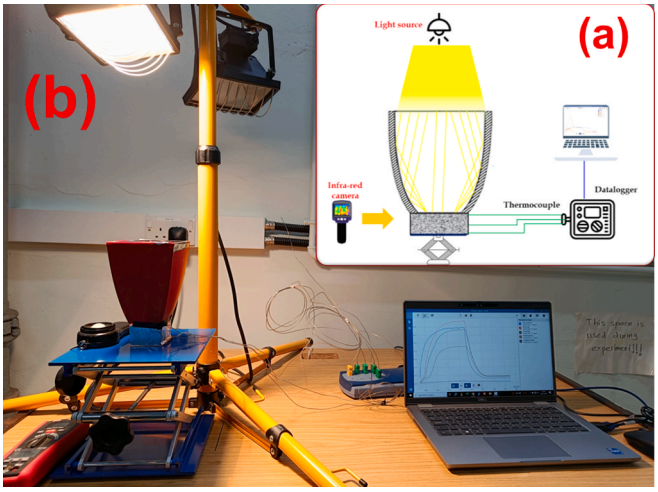


Fig. 8. Experimental setup, (a) Schematic; (b) Actual photograph.

with a reflective surface on the top side and insulating layer on the rear side.

3. Results and discussion

The material was initially characterised to determine the key thermal properties, including the phase transition temperature, the completion temperature of melting, and the heat of fusion. Following this, an extensive experimental investigation was conducted, examining the temperature distribution along the vertical axis of the cavity under both concentrated and non-concentrated conditions for RT28 and the composite. Additionally, the study includes an analysis of the effect of shading under concentrated radiation conditions.

3.1. Properties of composite

The important characteristics of the form stable composite of RT28 and softwood biochar are presented in Fig. 9. Functional groups and chemical compatibility between the PCM and supporting materials were identified using FTIR spectroscopy (JASCO system) over a wavenumber range of 600–4000 cm^{-1}. The FTIR plot (Fig. 9(a)) confirms the physical adsorption of RT28 into the cylindrical pores of the softwood biochar by capillary force without undergoing any chemical change. The FTIR spectra of softwood biochar displayed the characteristic aromatic peaks around 1500–1600 cm^{-1}, attributed to the stretching vibrations of aromatic C═C bonds in lignin-derived compounds. A distinct C═C stretching peak appeared near 1480 cm^{-1}, while weak bands at 740 cm^{-1} were assigned to C–H out-of-plane vibrations on aromatic rings. These features suggest the predominance of the physical adsorption mechanism, such as the capillary forces, Van der Waals interactions, and π–π electron donor–acceptor interactions between the PCM molecules and the biochar surface. This interaction preserves the crystalline structure of RT28 without the formation of new chemical bonds, which is crucial for maintaining its phase transition behaviour during thermal storage. The pristine PCM exhibited characteristic absorption bands at 2952 and 2846 cm^{-1} for the symmetric and asymmetric stretching of methylene and methyl groups, respectively, and the bending deformation bands at 1464 and 1377 cm^{-1}. The absence of new peaks in the composite spectrum confirms the successful physical impregnation of PCM into the porous biochar matrix [19].

The XRD plot (Fig. 9(b)) shows sharp peaks for softwood due to a presence of almost 90 % carbon [19]. The composite PCM displayed all the typical absorption peaks of the PCM, including distinct peaks associated with hydrocarbon absorption bands. The absence of new absorption peaks suggests that the supporting materials maintain the crystalline structure of RT28 without generating any new chemical groups. RT28 and composite also shows sharp peaks indicating the crystalline nature. It can be seen from the DSC result, as plotted in (Fig. 9 (c)), that the RT28 and composite have melting temperature of 25 °C

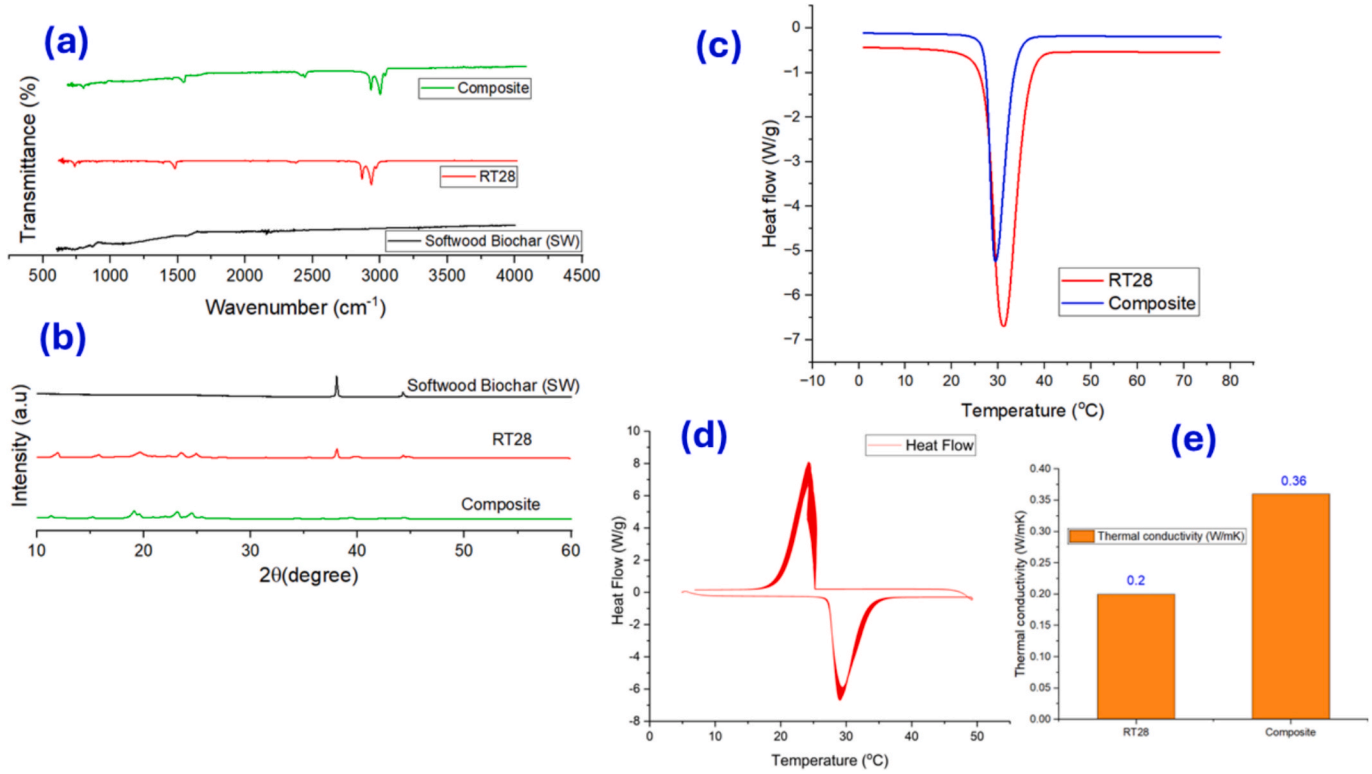


Fig. 9. Properties of composite and RT28, (a) FTIR; (b) XRD; (c) DSC plot; (d) Thermal cyclic test plot; and (e) Thermal conductivity [19].

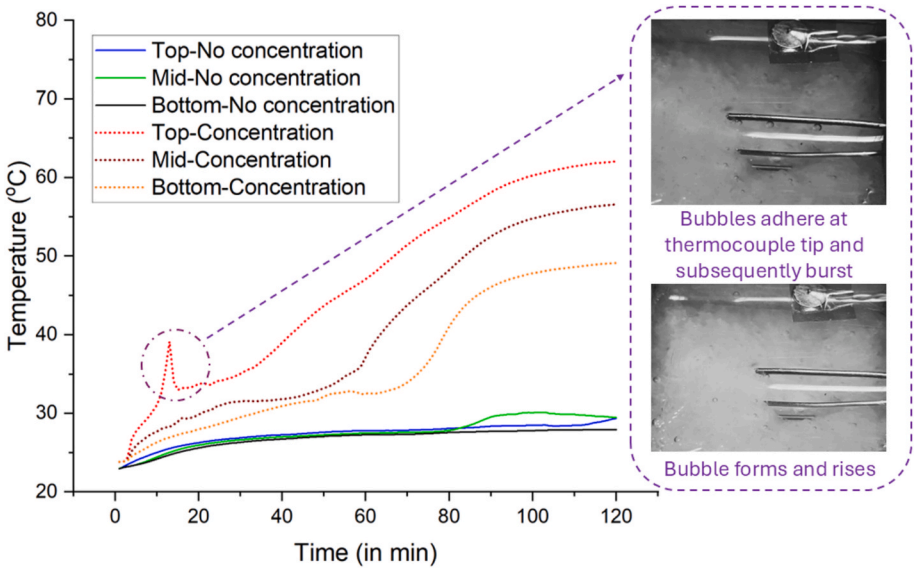


Fig. 10. Temperature variation at different depths along the cavity for RT28.

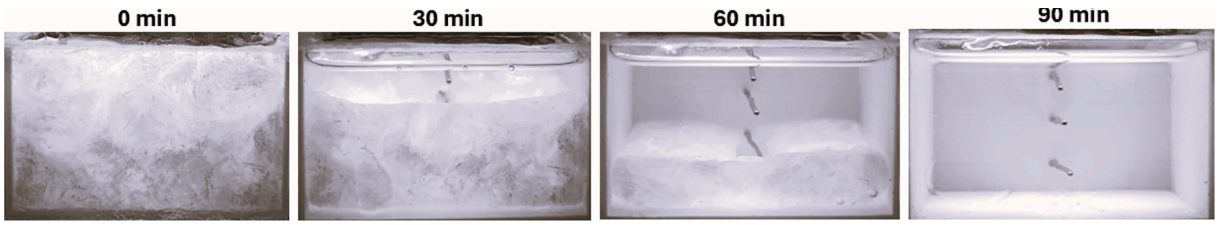


Fig. 11. Melting process of RT28.

and 26 °C respectively. The slightly higher temperature for the composite in comparison to the base PCM can be validated by the Clausius-Clapeyron relation [25–26]. The melting process is completed at a temperature of 40 °C and 37 °C for RT28 and composite, respectively. The reduced melting temperature range for the composite is due to the improved thermal conductivity, which is 80 % more than of the pure PCM. The latent heat of fusion for RT28 and the composite as calculated from the DSC curves is 228 J/g and 132 J/g respectively. There has been a 42 % reduction in the enthalpy of fusion in the case of the composite as compared to the pure RT28. This effect is primarily attributed to the carbonaceous biochar in the composite, which remains thermally stable without undergoing phase transformation during heat absorption. Additionally, the porous structure of the biochar restricts the molecular mobility of PCM during phase transition, leading to a reduction in heating enthalpy [27].

The composite has also been studied over 200 cycles of heating and cooling to find out the change in its thermal characteristics with aging. The change in case of the two key parameters i.e. latent heat of fusion and melting temperature is found to be negligible as can be seen from Fig. 9(d). There is only 3 % and 1 % reduction in the enthalpy of melting and solidification respectively for the aged composite over the new one. This confirms the reliability of the material to be used in applications requiring low maintenance and provide stable performance. Thermal conductivity is measured using the Hukesflux TPSYS20 thermal conductivity meter, equipped with a TP08 needle probe.

3.2. Temperature profiles

Fig. 10 shows the temperature along the depth of the cavity with RT28 as PCM. As the distance between the radiation source and the thermocouple position increase, the temperature decreases. The heat transfer is a little tricky in the case of paraffin wax. As the top layer receives the radiation and absorbs it, it gets heated up and melts once sensibly heated to its melting point. Followed by which a steady phase occurs till the entire PCM mass is melted. The melted layer now acts as an insulating sheet for the subsequent layers. This delays the melting the following layers as clearly seen from the Fig. 11 A peak has been observed in the temperature profile measured by the top thermocouple in the cavity near the melting temperature. The physics of bubble formation in paraffin (i.e. PCM) is quite fascinating. When PCM is heated, the molecules gain kinetic energy and begin to transition from the liquid to the gas phase. This transition occurs at the melting point, which is 26 °C under standard atmospheric pressure. As the PCM is further heated, small vapor bubbles form at the thermocouple surface (nucleation site). These initial bubbles are unstable and tend to collapse back into the liquid. When these bubble burst near the thermocouple surface releases energy locally and raises the temperature. As the process of bubble formation and collapse ceases, the temperature profile back to normal and follows the usual trend as can be seen from Fig. 10. Understanding the physics of bubble formation is important in various applications, such as the design of efficient heating systems, the understanding of boiling heat transfer, and the study of multiphase flows in engineering and scientific research.

When the cavity is filled with composite and studied under the concentration and non-concentration conditions, it was observed that the temperature rise is found to be far higher in the cavity with composite as compared to cavity with RT28. It is clearly seen that temperature is directly proportional to the value of incoming radiation. At the highest point, the temperature recorded by thermocouple at the top section of the cavity reaches a maximum of 107.8 °C and 53 °C under the concentration and non-concentration conditions, this is 103 % more. The trend of temperature change is similar in each case. The slope is

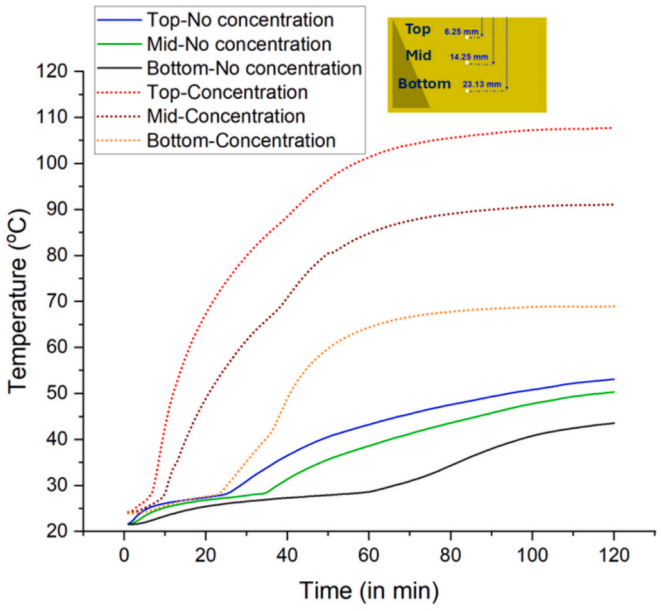


Fig. 12. Temperature variation at different depths for the cavity with form stable composite.

gentle in the case of the RT28 after phase transition is complete, wherein for the composite a steep slope can be observed. The range of temperature reduces as the distance between the location of measurement and source increases. In both the samples, the consistent temperature gradient indicates a clear downward heat transfer, confirming that the heat from the top source is moving downward as anticipated.

An important conclusion also can be drawn from Fig. 12, the duration for the melting process also significantly reduced when concentrator is integrated to the thermal energy storage cavity with composite. The melting time computed for the top section of the composite in the cavity with and without the concentrator is 32 min and 5 min respectively, thus with concentrator the melting process is completed 5.4 times faster than without any concentration arrangement. This result is significant from practical applications point of view, such integrated arrangement can be very helpful in the regions where both irradiance and duration of sunshine is low.

Fig. 13 presents the variation of temperature in the midsection of the cavity with composite under concentrated and non-concentrated conditions. At all three levels the temperature for the composite much higher than the temperature of RT28 at the highest level. Temperature for the concentrating condition is observed to be higher than the non-concentration conditions with a quicker melting process. The average temperature for the composite at level 3, 2 and 1 are 89.7 °C, 73.8 °C and 54.8 °C, respectively. While for RT28 the average temperature is 40.7 °C at level 3. This temperature variation can be explained based on influence of latent heat and sensible heat in each material. In the pure PCM, most of the stored energy is attributed to latent heat. Similarly, in the composite material, the latent heat of the PCM remains the dominant mode of energy storage. This is followed by a comparatively smaller contribution from the sensible heat of the PCM, along with an additional contribution from the sensible heating of the biochar. These findings indicate that the inclusion of biochar in the composite not only facilitates a more uniform temperature distribution but also enhances thermal conductivity, leading to increased energy storage within the same time frame. While the pure PCM possesses a higher latent energy storage capacity, the faster melting rate and form-stability provided by the biochar composite are more critical for applications in latent heat thermal energy storage systems.

As it is evident from the Fig. 14 natural convection is dominant means of heat transfer in the cavity when RT 28 is used. Using a composite material helps suppress convection, which aids in enhancing the uniformity of the temperature field in the gravitational direction. Natural convection in this system arises due to two primary physical mechanisms. Firstly, due to temperature difference and buoyancy force. The temperature variation within the PCM leads to differences in density. Specifically, the higher-temperature region of the melted PCM has a lower density compared to the cooler, higher-density regions. The less dense, warmer material tends to rise, while the denser, cooler material sinks, creating a local circulation flow. This flow is driven by buoyancy forces, which arise because of the density differences within the PCM. Essentially, the fluid in hotter regions becomes lighter, and as it moves upwards, the cooler, denser fluid takes its place, establishing a convection current. The second mechanism is volume expansion and pressure gradient. When paraffin melts, it undergoes thermal expansion, meaning its volume increases. This expansion creates a pressure gradient within the material: the increased volume in the hotter, melted regions causes a local pressure rise, which drives the melted paraffin upwards. This pressure difference further contributes to the upward movement of the molten material, assisting the overall convection process [28].

The presence of the softwood biochar porous network significantly reduces the impact of natural convection. In summary, the RT28 sample without carbonaceous biochar struggles to maintain a desirable condition on the top surface of the cavity exposed to incoming radiation, leading to lower and uneven temperatures. This makes its effectiveness in thermal control questionable. The primary issue is that excessive heat accumulates at the top wall as sensible heat, causing significant natural convection, a non-uniform temperature field, and severe thermal

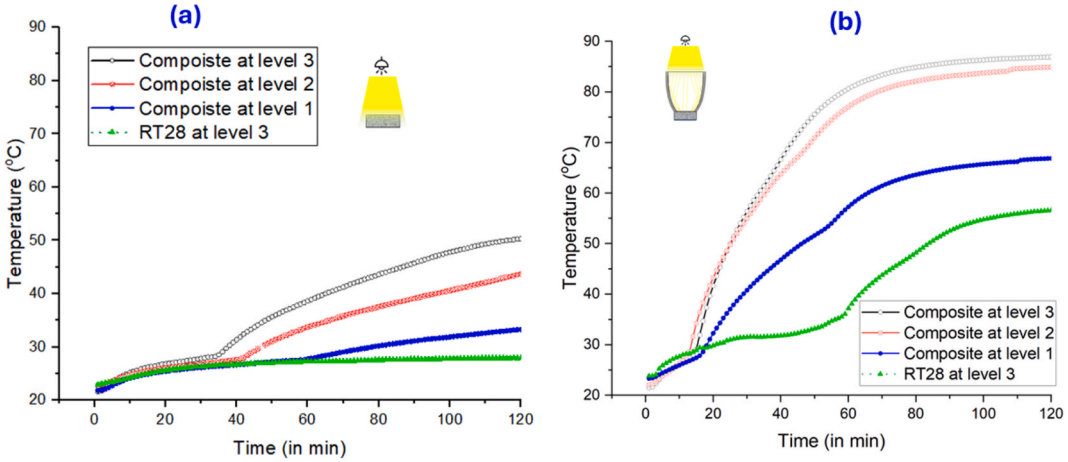


Fig. 13. Temperature at the midsection of cavity at different radiation; (a) under no-concentration, (b) under concentration.

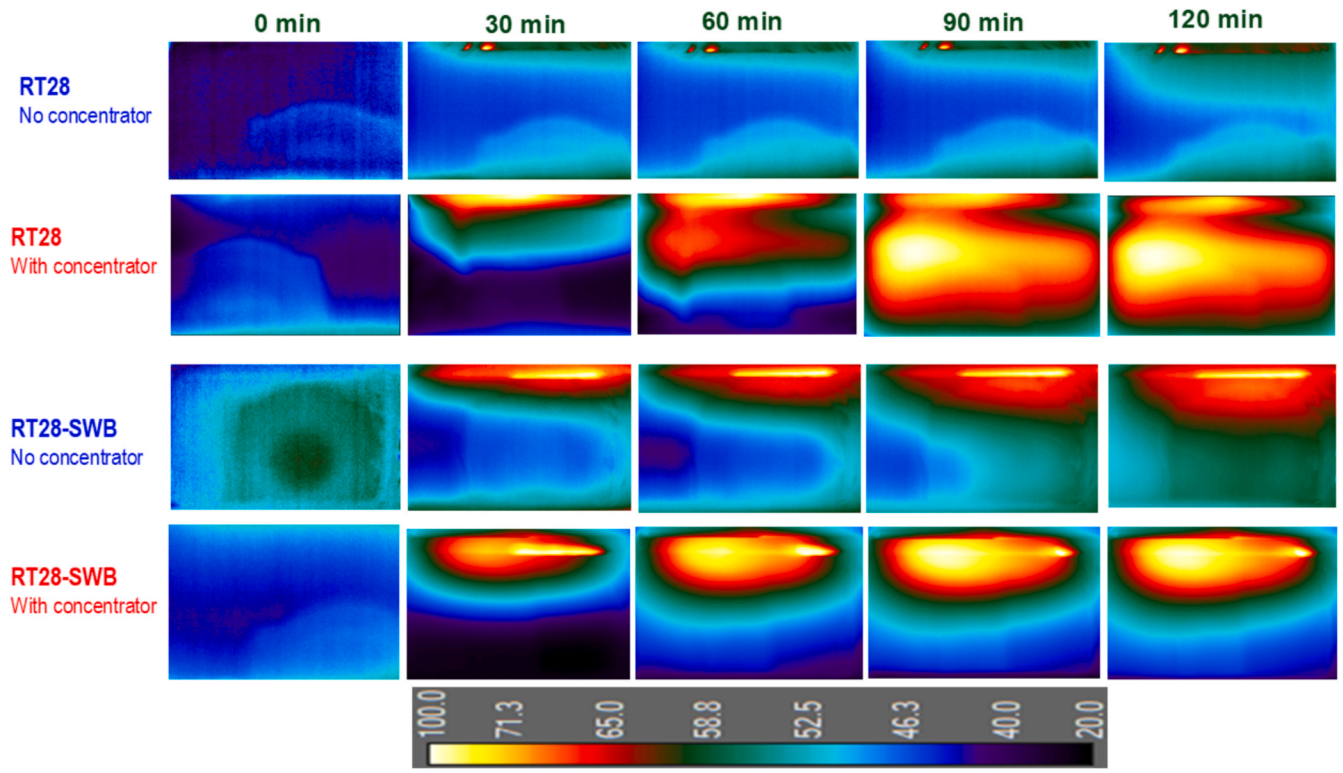


Fig. 14. Temperature contours for RT28 and composite PCM under concentration and non-concentration conditions.

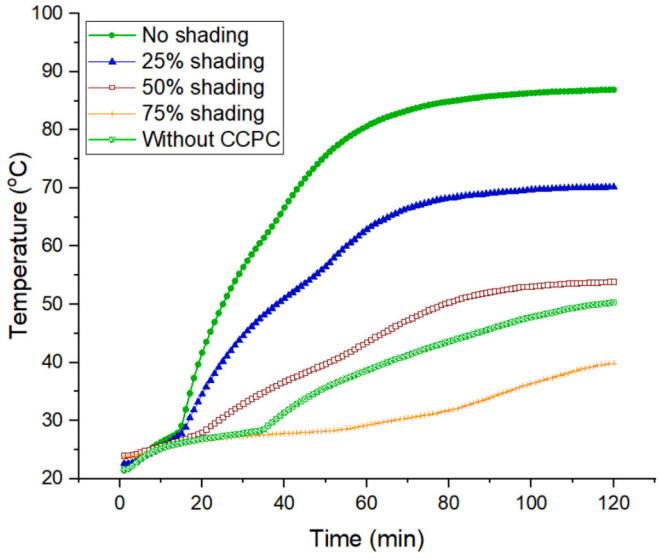


Fig. 15. Effect of shading on the temperature profile for the composite PCM.

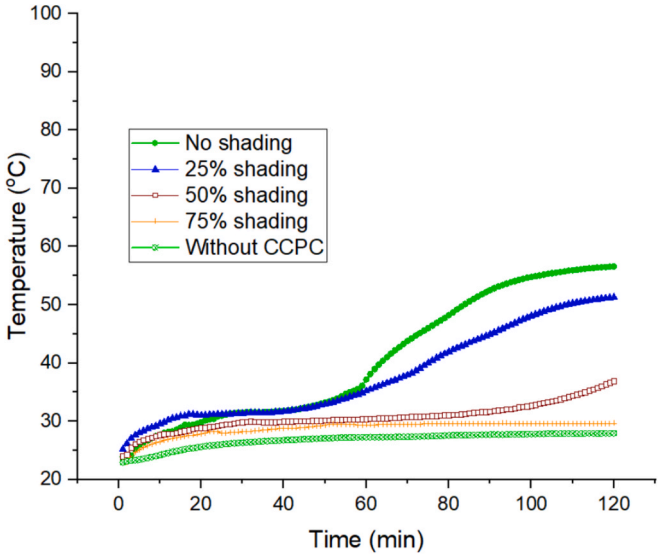


Fig. 16. Effect of shading on the temperature profile for RT28.

stratification. Instead of being quickly and uniformly stored as latent heat throughout the phase change unit, this leads to uneven phase change and temperature distribution, as well as higher heating source temperatures. For effective thermal management, the composite material is strongly recommended, as it efficiently transfers heat from the top to the bottom, ensuring uniform distribution and preventing significant thermal hot spots in the cavity. This is crucial for the longevity of the cavity material and adds substantial economic value in practical applications.

3.3. *Shading experiment*

This study has a great significance from application point. As seen from Figs. 15 and 16, with increase in the fraction of blockage of entry area of the concentrator, the temperature of the material in cavity decreases. The temperature of the material with maximum shading (75 %) is still higher than the case where no concentration was used. The average temperature in case of the composite is 73.8 °C with the use of the concentrator under no shading condition. When 25 % of the entry area of the concentrator is covered to block incoming radiation, the average temperature of the composite in the cavity reduces to 55.5 °C. This temperature further reduces to 42 °C and 30 °C, when shading

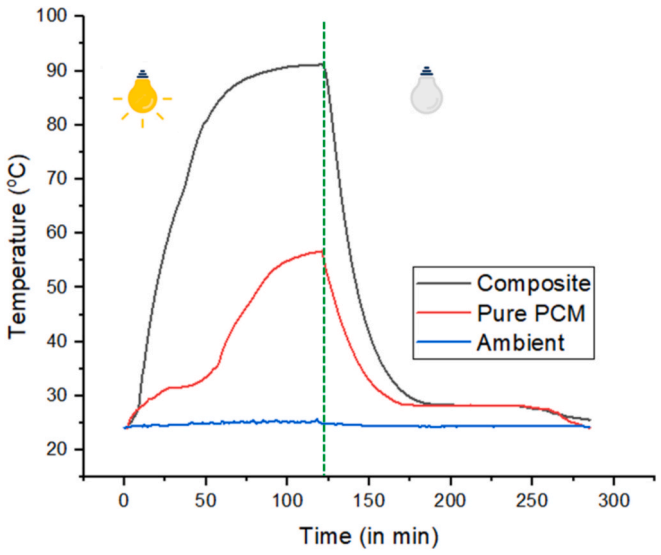


Fig. 17. Photothermal conversion performance curve.

increases to 50 % and 75 % respectively. The melting time also increases from 9 min to 10 under no shading and 25 % shading conditions. The melting time significantly increases to 87 min when the shading of the concentrator is 75 %. The average temperature is 38 °C, 30.7 °C and 28.7 °C for RT28 with 25 %, 50 % and 75 % shading respectively. This study confirms that a well-designed sun-tracking mechanism if integrated to CPCC-TES system can significantly impact the performance. But a low shading below 25 % found to have minimal effect on melting time but it has clear impact on the temperature range of the material.

Fig. 17 shows the charging and discharging curve of RT28 and softwood biochar-based composite. Both charging and discharging in case of pure PCM is seen to be slow as that of the composite. The temperature–time curve shows a single plateau in the time range of 5–58 min (temperature range 26–37 °C) for the pristine PCM. In the case of the composite, the length of the plateau is much shorter than that of the pristine PCM. After these stable plateaus, the temperature rises in each case. However, the slope of temperature rise is found to be steep in the case of the composites than that of the pristine PCM. The temperature increases and reaches 56.6 °C and 87 °C for RT28, and composite, respectively.

Once the light source was turned off, the temperature dropped rapidly. The temperature reaches 28.6 °C for the composite from its peak in 68 min, whereas for RT28 it took 54 min to reach 28 °C. During the cooling phase, wider plateau has been observed for pure PCM in the time range of 174–264 min compared to the time range of 189–242 min for composite. After the plateau region the temperature of the samples reach thermal equilibrium with ambient.

In this study the value of radiation has been fixed at 2000 W/m^2. It can be seen from the Fig. 17, the melting process for RT28 and composite starts at 3 min, and 1 min respectively. The melting completion takes approximately 3 min and 17 min for the composite and the pure PCM, respectively. Therefore, the value of photothermal conversion efficiency is evaluated to be 30 % and 81 % respectively for RT28 and softwood composite. The results indicate that the composites significantly outperform pure PCM in converting solar energy into latent heat. This enhancement in photothermal conversion and storage efficiency is primarily due to the elevated optical absorptivity of the softwood-derived biochar, which markedly improves solar absorption. These findings highlight the promise of the form-stable biochar-based composite for advanced solar thermal energy storage applications.

Table 2 presents a comparative analysis of crucial parameters for both the form stable composite and RT28 desirable for TES applications. The time of melting and temperature presented in the table is calculated from the data recorded by thermocouple placed in the mid-section of the cavity.

4. Conclusions

Visualisation and measurement experiments were carried out in this work for the melting process of biochar-PCM form stable composite undergoing solid–liquid phase change. A cavity filled with the developed material has been studied with a cross compound parabolic concentration device integrated to augment the irradiance on the storage media. From this experimental, it has been observed that the form stable material produced has better thermal characteristics as that of the pure PCM and the material shows tremendous potential for direct solar absorption when a low-cost concentration arrangement is made. Such integrated and simplified solar energy harvesting device could be a gamechanger in the field of low temperature energy storage for domestic applications. Some of the significant findings are presented as follows.

1. A blend of softwood biochar with the surface area of 441 m^2/g and RT28 in weight ratio 1:1 is suitable to contain the leakage and improve the thermal characteristics.
2. The CCPC designed with an optical concentration ration of 3.7 is found optimal for integration into direct absorption thermal energy storage system with form-stable composite.
3. The melting time of the composite with CPCC is 5.4 times faster than without any concentration arrangement. It indicates that a TES with

Table 2
Comparison of melting temperature, maximum temperature and unit mass energy storage time.

Cases	Melting temperature (°C)	Melting completion temperature(°C)	Full melting time (s),t_m	Maximum temperature (°C)	Mass energy storage time (s/m^3),C_m [29] $C_m = \frac{t_m}{V_{PCM}}$ Here, V_{PCM} is volume of the PCM material in the cavity
Composite- non concentration (L1)	26	37	–	33.3	–
Composite- non concentration (L2)	26	37	3480	43.7	4.7×10^7
Composite- non concentration (L3)	26	37	2460	50.3	3.3×10^7
Composite-concentration (L1)	26	37	840	66.9	1.1×10^7
Composite- concentration (L2)	26	37	480	84.9	6.5×10^6
Composite- concentration (L3)	26	37	420	86.9	5.6×10^6
RT28- non concentration (L3)	25	31	–	27.9	–
RT28- concentration (L3)	25	31	3600	56.6	5.1×10^7

CPCC can be efficient solution for widescale implementation of PCM based TES where the sunshine hours is low.

4. At an irradiance of 540 W/m^2, the composite based TES integrated with CPCC can store thermal energy at an average temperature of 89.7 °C. This is 120 % improvement as that of the TES without CPCC. This is significant as thermal energy at higher temperature is more useful. It is also evident from this fact that TES-CPCC integrated solar thermal conversion system can be useful solution in the areas where solar irradiance level is low and sunshine hour window is narrow.
5. Shading of the concentrator entry area found to have significant impact on the average temperature of the composite in the rectangular cavity. A shading of 25 % entry area can reduce the average temperature by 24.8 °C compared to non-shading conditions.

Though this study presented some of the key findings, still there are areas which need to be explored in depth. Developing form stable material with biochar that could operate in high temperature application will be significant breakthrough, as with installation of large scale Concentrated Solar Plant efficient storage technologies and materials are in high demand. Digital twin integration with such TES systems could be beneficial intervention in acquiring real time feedback and improving the design of the system.

CRediT authorship contribution statement

Dudul Das: Writing – original draft, Methodology, Formal analysis, Conceptualization, Data curation, Investigation, Software, Validation, Visualization, Writing – review & editing. **Manosh C. Paul:** Writing – review & editing, Supervision, Project administration, Funding acquisition, Conceptualization, Resources.

Declaration of competing interest

The authors declare the following financial interests/personal relationships which may be considered as potential competing interests: Manosh Paul reports financial support was provided by UK Research and Innovation. Dudul Das reports financial support was provided by UK Research and Innovation. If there are other authors, they declare that they have no known competing financial interests or personal relationships that could have appeared to influence the work reported in this paper.

Acknowledgements

The study is supported by EU MSCA Fellowship (101063361) and EPSRC, UK under grant EP/X027783/1. The authors also wish to recognise support from the UKRI Supergen Bioenergy Impact Hub (EP/Y016300/1). The biochar was provided by the UK Biochar Research Centre at the University of Edinburgh [18].

Appendix A. Supplementary data

Supplementary data to this article can be found online at https://doi.org/10.1016/j.solener.2025.113609.

Data availability

The data that support the findings of this study is available in the Supplementary File.

References

[1] D. Das, P. Kalita, O. Roy, Flat plate hybrid photovoltaic- thermal (PV/T) system: A review on design and development, Renew. Sustain. Energy Rev. 84 (2018) 111–130, https://doi.org/10.1016/j.rser.2018.01.002.
[2] P. Kalita, S. Das, D. Das, P. Borgohain, A. Dewan, R.K. Banik, Feasibility study of installation of MW level grid connected solar photovoltaic power plant for northeastern region of India, Sādhanā 44 (2019) 207, https://doi.org/10.1007/s12046-019-1192-z.
[3] A. Sharma, V.V. Tyagi, C.R. Chen, D. Buddhi, Review on thermal energy storage with phase change materials and applications, Renew. Sustain. Energy Rev. 13 (2009) 318–345, https://doi.org/10.1016/j.rser.2007.10.005.
[4] G. Li, Y. Hwang, R. Radermacher, Review of cold storage materials for air conditioning application, Int. J. Refrig 35 (2012) 2053–2077, https://doi.org/10.1016/j.ijrefrig.2012.06.003.
[5] D. Das, R. Crosby, M.C. Paul, A comprehensive review on the form stable phase change materials for storing renewable heat preparation, characterization and application, J Energy Storage 110 (2025) 115284, https://doi.org/10.1016/j.est.2024.115284.
[6] K. Liu, Z.F. Yuan, H.X. Zhao, C.H. Shi, F. Zhao, Properties and applications of shape-stabilized phase change energy storage materials based on porous material support—A review, Mater. Today Sustainability 21 (2023) 100336, https://doi.org/10.1016/j.mtsust.2023.100336.
[7] M.Q. Wu, S. Wu, Y.F. Cai, R.Z. Wang, T.X. Li, Form-stable phase change composites: Preparation, performance, and applications for thermal energy conversion, storage and management, Energy Storage Mater. 42 (2021) 380–417, https://doi.org/10.1016/j.ensm.2021.07.019.
[8] C. Qiu, H. Jiang, P. Liu, C. Jiang, X. Ji, Y. Zhang, W. Sun, X. Guo, An ultrastrong wood-based phase change material for efficient photothermal conversion and thermal energy conservation, Compos. B Eng. 279 (2024) 111460, https://doi.org/10.1016/j.compositesb.2024.111460.
[9] C. Sarkar, A. Bhattacharya, T.B. Ashagre, R. Verma, D. Rakshit, S. Saha, Facile fabrication of shape-stable phase change materials based green composite for passive conditioning in buildings, Renew Energy 247 (2025) 122946, https://doi.org/10.1016/j.renene.2025.122946.
[10] H. Li, R.Y. Tay, S.H. Tsang, R. Hubert, P. Coquet, T. Merlet, J. Foncin, J.J. Yu, E.H. T. Teo, Thermally conductive and leakage-proof phase-change materials composed of dense graphene foam and paraffin for thermal management, ACS Appl. Nano Mater. 5 (2022) 8362–8370, https://doi.org/10.1021/acsanm.2c01462.
[11] P. Liu, Z. Tan, X. Cui, Z. Zhang, H. Fang, H. Li, L. Bian, X. Gu, Comparative study of different typical organic form-stable phase change materials packaged by carbonized wheat straw-expanded graphite binary supporting material, J. Energy Storage 108 (2025) 115088, https://doi.org/10.1016/j.est.2024.115088.
[12] D.G. Atinafu, B. Yeol Yun, Y. Uk Kim, S. Wi, S. Kim, Introduction of eicosane into biochar derived from softwood and wheat straw: Influence of porous structure and surface chemistry, Chem. Eng. J. 415 (2021), https://doi.org/10.1016/j.cej.2021.128887.
[13] D. Das, U. Bordoloi, H.H. Muigai, P. Kalita, A novel form stable PCM based bio composite material for solar thermal energy storage applications, J. Energy Storage 30 (2020) 101403, https://doi.org/10.1016/j.est.2020.101403.
[14] E.F. Akyurek, M. Yoladi, An experimental investigation on melting and solidification behavior of phase change material in cylindrical latent heat storage units with minichannel, J. Energy Storage 41 (2021), https://doi.org/10.1016/j.est.2021.102938.
[15] V. Joshi, M.K. Rathod, Thermal transport augmentation in latent heat thermal energy storage system by partially filled metal foam: A novel configuration, J. Energy Storage 22 (2019) 270–282, https://doi.org/10.1016/j.est.2019.02.019.
[16] S. Zhang, L. Pu, S. Mancin, Z. Ma, L. Xu, Experimental study on heat transfer characteristics of metal foam/paraffin composite PCMs in large cavities: Effects of material types and heating configurations, Appl Energy 325 (2022) 119790, https://doi.org/10.1016/j.apenergy.2022.119790.
[17] R. Crosby, D. Das, M.C. Paul, Numerical study and experimental validation of a porous biochar supported form stable composite for thermal energy storage, J. Energy Storage 99 (2024) 113314, https://doi.org/10.1016/j.est.2024.113314.
[18] O. Mašek, P. Brownsort, A. Cross, S. Sohi, Influence of production conditions on the yield and environmental stability of biochar, Fuel 103 (2013) 151–155, https://doi.org/10.1016/j.fuel.2011.08.044.
[19] D. Das, O. Masek, M.C. Paul, Development of novel form-stable PCM-biochar composites and detailed characterization of their morphological, chemical and thermal properties, J. Energy Storage 84 (2024) 110995, https://doi.org/10.1016/j.est.2024.110995.
[20] R. Yang, X. Guo, H. Wu, W. Kang, K. Song, Y. Li, X. Huang, G. Wang, Anisotropic hemp-stem-derived biochar supported phase change materials with efficient solar-thermal energy conversion and storage, Biochar 4 (2022) 38, https://doi.org/10.1007/s42773-022-00162-1.
[21] M. Al-Shidhani, M. Gao, Improving angular response of crossed compound parabolic concentrators using rectangular entry aperture, Renew Energy 204 (2023) 1–10, https://doi.org/10.1016/j.renene.2022.12.104.
[22] M. Khalid, J. Wei, S. Bakhsh, M.A. Qaisrani, M. Sohail, J. Fang, Comparative optical performance investigation of Cross Compound Parabolic Concentrators designed with the elimination of multiple reflections principle, Sol. Energy 258 (2023) 253–269, https://doi.org/10.1016/j.solener.2023.04.064.
[23] F. Masood, P. Nallagownden, I. Elamvazuthi, J. Akhter, M.A. Alam, A new approach for design optimization and parametric analysis of symmetric compound parabolic concentrator for photovoltaic applications, Sustainability 13 (2021), https://doi.org/10.3390/su13094606.
[24] S, P.B.D., Ganapathiraman, S., Manikam, P., 2023. Design procedure of stationary compound parabolic concentrator with flat plate absorber for effective year-round performance – Response Surface Methodology and Tracepro as tools. Cleaner Energy Syst. 5, 100074. doi: 10.1016/j.cles.2023.100074.
[25] Z. An, H. Chen, X. Du, T. Shi, D. Zhang, Preparation and performance analysis of form-stable composite phase change materials with different EG particle sizes and

mass fractions for thermal energy storage, ACS Omega 7 (2022) 34436–34448, https://doi.org/10.1021/acsomega.2c04101.
[26] P. Lv, C. Liu, Z. Rao, Experiment study on the thermal properties of paraffin/kaolin thermal energy storage form-stable phase change materials, Appl. Energy 182 (2016) 475–487, https://doi.org/10.1016/j.apenergy.2016.08.147.
[27] D.G. Atinafu, S. Jin Chang, K.-H. Kim, S. Kim, Tuning surface functionality of standard biochars and the resulting uplift capacity of loading/energy storage for organic phase change materials, Chem. Eng. J. 394 (2020) 125049, https://doi.org/10.1016/j.cej.2020.125049.
[28] X. Yang, P. Wei, X. Cui, L. Jin, Y.-L. He, Thermal response of annuli filled with metal foam for thermal energy storage: an experimental study, Appl Energy 250 (2019) 1457–1467, https://doi.org/10.1016/j.apenergy.2019.05.096.
[29] Z. Du, X. Huang, Y. Li, G. Liu, X. Yang, B. Sundén, Experimental study on melting and solidification cycle of a hybrid pin fin/metal foam energy storage tank, ASME J. Heat Mass Transfer 146 (2024), https://doi.org/10.1115/1.4065349.